Redistribution and Dilatation Effects in Turbulent Premixed Opposed Jet Flames

L. Tian, R. P. Lindstedt*

Department of Mechanical Engineering, Imperial College London, Exhibition Road, London SW7 2AZ, UK.

Abstract

Turbulent premixed opposed jet flames typically feature large density variations coupled with an imposed pressure gradient, both affect turbulence and scalar statistics significantly. The present work explores the modelling of such flames at the full second moment level for both velocity and scalar transport and includes extended variable density forms for redistribution/scrambling, dilatation and dissipation. The full closure includes preferential acceleration and dilatation models and is applied to the simulation of lean methane–air flames with the thermochemistry derived for the laminar flamelet regime. The encouraging agreement with experimental data for both turbulence and scalar quantities illustrates the importance of dilatation effects with the extended closure providing significantly improved agreement. However, it is also noted that the treatment of redistribution appears inaccurate near the stagnation plane. Furthermore, an analysis of the modelled scalar flux equation reveals that the treatment of "dilatation" and the mean scalar gradient has a significant impact and that the modelling of scalar dissipation requires further attention. Comparisons for a flame close to the flammability limit suggests that the current flamelet assumption is insufficient to capture the extinction.

1. Introduction

Second moment closure methods [1, 2] provide higher accuracy for turbulence and scalar statistics compared to the eddy viscosity formalism (e.g. the k-ϵ model [3]), which, for example, fails to predict non–gradient transport [4]. Experiments on opposed jet flows [5, 6] provide canonical test cases for the assessment of closure approximations and recent studies [6] of lean premixed flames feature fractal–grids to generate turbulence at comparatively high Reynolds numbers in order to reduce the relative effect of bulk strain. In addition to the mean and turbulence quantities, turbulent scalar fluxes are now also available for comparisons with computational studies.

The modelling of pressure–related terms is a key issue for the closures of second moment methods. Such terms also tend to act across scales and an understanding of their importance is of relevance also to Large Eddy Simulation (LES) based simulations [7]. The large density variations in opposed jet flames bring further difficulties as variable density effects should be considered. This inherent characteristic makes the prevalent density weighed form [1] of redistribution/scrambling models insufficient [2]. The variable density effects mainly function in two ways and are included in the mean pressure gradient terms and pressure-strain terms, respectively. The former relates to the preferential acceleration effects driven by the mean pressure gradient. The corresponding acceleration extensions [2] are independent of the combustion regime and have been successfully added to extend isothermal redistribution/scrambling models. The other variable density effect is associated with the fluctuating pressure, which requires additional models for scrambling in the scalar flux transport and for dilatation in the transport of Reynolds stresses. Dilatation models (e.g. [8, 9]) have seldom been used in the context of second moment closures due to formulation and implementation difficulties.

The objective of the present study is to test a complete closure for the pressure correlation terms for premixed turbulent flames and explore the possible need for further developments for turbulence and chemistry closures. A class of model extensions associated with preferential acceleration effects as well as "dilatation" effects have been added to the isothermal counterparts in Reynolds stress, scalar flux and turbulent kinetic energy dissipation equations, respectively. The chosen dilatation model is consistent of the reaction–related closure implied by the BML formalism [10]. The extended complete closure is applied to the simulation of lean premixed turbulent methane–air opposed jet flames. Comparison with both mean and fluctuating quantities are made, including the turbulent scalar flux.

2. Closure Approximations

The starting point of the current study is a full second moment closure for both velocity and scalar fields [2]. The formulation includes extended forms for redistribution and scrambling terms. However, the "dilatation" effects, induced by the fluctuating pressure, were not added, but have been included here. Such terms can be significant for combusting flow with large density variations and the dilatation model is using a formalism [9] that is consistent with a reaction rate closure for the laminar flamelet regime of combustion. The corresponding term associated with the divergence of the fluctuating scalar shares a similar form,

$$\phi_{ij}^{D} = \frac{1}{3}\delta_{ij}\left(\tau u_L\right)^2\overline{S_c}\Big(\langle c\rangle - \frac{1}{2}\Big) \tag{1}$$

$$\phi_{ic}^{S_e} = \frac{1}{2}\left(\tau u_L\right)\overline{S_c}\Big(\langle c\rangle - \frac{1}{2}\Big) \tag{2}$$

where $\langle\,\cdot\,\rangle$ represents the conventional average form with τ, u_L and $\overline{S_c}$ represent the expansion ratio, laminar burning velocity and mean reaction rate, respectively.

The dilatation/extended scrambling terms induced by the fluctuating pressure are exact in both transport equations of Reynolds stress and scalar flux. However, a modelled term is added into the $\widetilde{\epsilon}$ equation with a coefficient C_{ϵ_4}. The constant should be of order unity and the impact on the modelling of the current flames is discussed below.

The common absence of scaling effects based on the mean scalar gradient is another issue. Thus in addition to the preferential acceleration ϕ_{ic}^{A} and dilatation/extended scrambling $\phi_{ic}^{S_e}$ terms, the present study analyses the effects of an additional scrambling term to balance the production of scalar flux [12]. Accordingly, the scrambling term $\phi_{ic}^{S_s}$ replaces the isothermal counterpart in Table 1 and takes the following form:

* Corresponding author: p.lindstedt@imperial.ac.uk

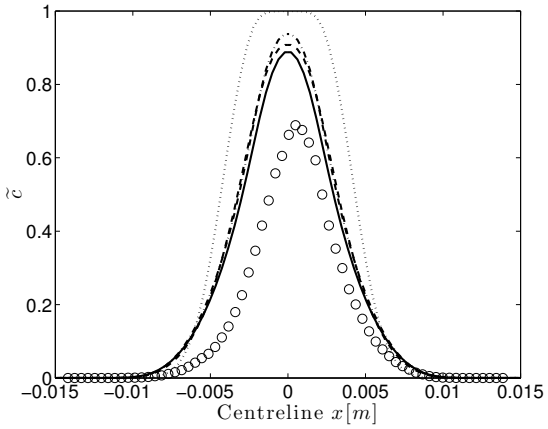

Figure 1: Predicted and measured mean reaction progress variable ($\widetilde{c}$) along the centreline. Symbols: ($\circ$) experimental data ($\phi = 0.90$) by Goh et al. [6]. Lines: (—) SMC with dilatation model and standard dissipation equation; (-··-) SMC with dilatation model and the modified dissipation equation [14]; (- - -) SMC without dilatation model [2]; ($\cdots$) k-ϵ model.

$$\phi_{ic}^{S_s} = -C_{1c}R_\tau \frac{\widetilde{\epsilon}}{\widetilde{k}}\widetilde{u_i''c''} + C_{2c}\widetilde{u_i''c''}\frac{\partial \widetilde{U_i}}{\partial x_j} + C_{3c}\left(\widetilde{u_i''u_k''} - \frac{2}{3}\delta_{ik}\widetilde{k}\right)\frac{\partial \widetilde{c}}{\partial x_k} \quad (3)$$

The model constants are $R_\tau = 0.8$, $C_{1c} = 3.0$, $C_{2c} = 0.5$ and $C_{3c} = 0.25$ [12].

The diffusion terms, such as the triple moments, which have a minor impact, are modelled using the generalised gradient diffusion model of Daly and Harlow [13]. The turbulent kinetic energy dissipation is normally based on the "standard" dissipation equation [11]. However, the renormalization group form developed by Yakhot and Orszag [14] has also been examined. The chemical reaction rate closure follows the two–scale formulation by Lindstedt and Váos [2]:

$$\overline{S_c} = C_R\rho_u \frac{u_L}{v_K}\frac{\widetilde{\epsilon}}{\widetilde{k}}\widetilde{c}\left(1-\widetilde{c}\right) \quad (4)$$

where the reaction rate constant $C_R = 2.6$. The complete closure is listed in Table 1.

3. Application of the Model

The full closure was applied to the simulation of the lean ϕ = 0.80 and 0.90 turbulent premixed methane–air opposed jet flames investigated experimentally by Goh et al. [6]. For the richer flame, the laminar burning velocity (u_L) and the heat release parameter (τ) were obtained as 0.325 ms^{-1}and 5.720 [15] and for the leaner case the corresponding values were 0.262 ms^{-1} and 5.407. Simulations were performed using a two-dimensional axi–symmetric approximation and were fully transient with the governing equations integrated in a conservation form. The computational domain was discretised using a uniform orthogonal 190×39 cells (radial×axial). Grid-independence was verified with the same aspect ratio, but with 60 grids applied in the burner axial direction. The grid spacing was set to be similar to the experimentally estimated Kolmogorov scale [16] in the cold flow. A variable predictor–corrector variant (with splitting error control) of the PISO [17]

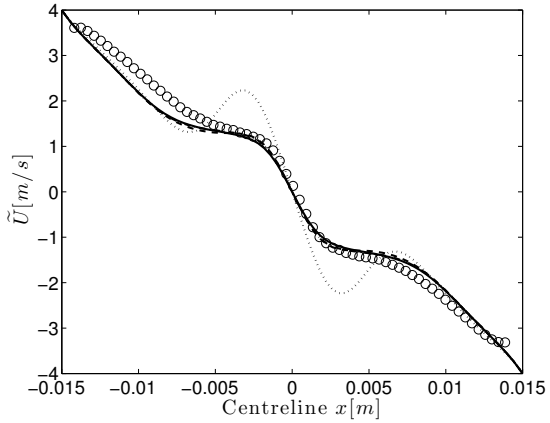

Figure 2: Predicted and measured mean velocity ($\widetilde{U}$) along the centreline. Symbols and lines as in Fig. 1.

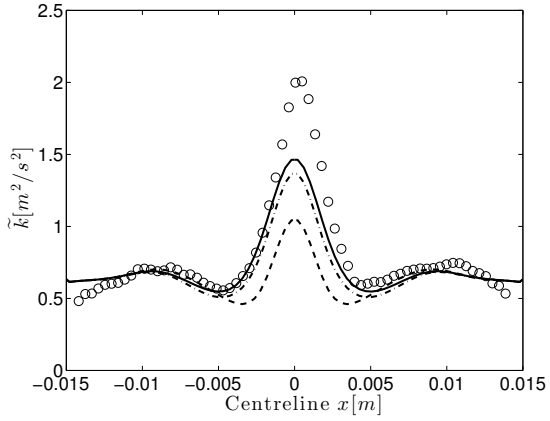

Figure 3: Predicted and measured turbulent kinetic energy ($\widetilde{k}$) along the centreline. Symbols: ($\circ$) experimental data ($\phi = 0.90$) by Goh et al. [6]. Lines: (—) SMC with dilatation model and standard dissipation equation; (-··-) SMC with dilatation model and the modified dissipation equation [14]; (- - -) SMC without dilatation model [2].

.

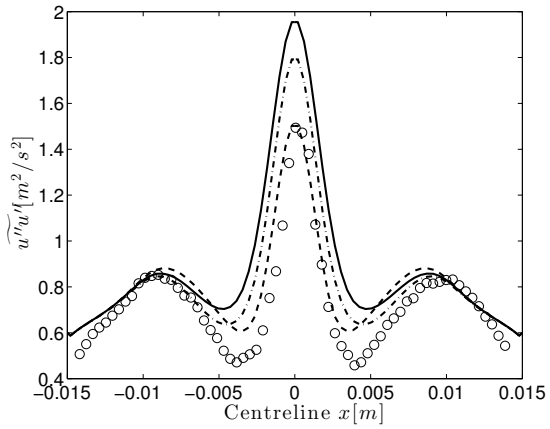

Figure 4: Predicted and measured axial Reynolds stress ($\widetilde{u''u''}$) along the centreline. Symbols and lines as Fig. 3.

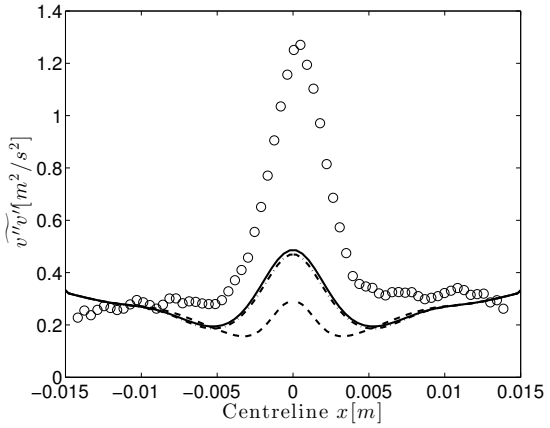

Figure 5: Predicted and measured radical Reynolds stress ($\widetilde{v''v''}$) along the centreline. Symbols and lines as Fig. 3.

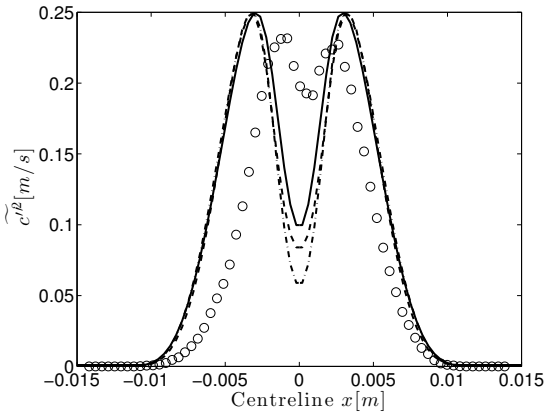

Figure 6: Predicted and measured scalar variance ($\widetilde{c''^2}$) along the centreline. Symbols and lines as Fig. 3.

algorithm was applied for the velocity-pressure coupling. A TVD scheme [18] was used to reduce numerical diffusion [2].

3.1 Closures

For comparison, the results obtained with the k-ϵ model are presented along with the full second moment closures proposed by Lindstedt and Váos [2] and, finally, with the current "dilatation models". To be consistent with the simulation results, the experimental data has been converted into Favre averaging form according to the BML theory [10].

Predicted and measured mean reaction progress variable and velocity along the centreline are shown in Figs. 1 and 2 for the case with $\phi = 0.90$. Inspection of Fig. 1 reveals that full second moment closures capture the position of flame front and the thickness of flame brush reasonably accurately, while the k-ϵ model cannot. As shown in Fig. 2, excellent agreement for the mean velocity is obtained along the centreline for the full second moment closures. The addition of the "dilatation" model provides slightly better agreement. The modified dissipation equation [14] has a comparatively minor impact on mean quantities and slightly increases the mean reaction progress variable.

3.2 Effects of Dilatation

The effects of "dilatation" model have been further examined for both turbulence and scalar quantities as shown in

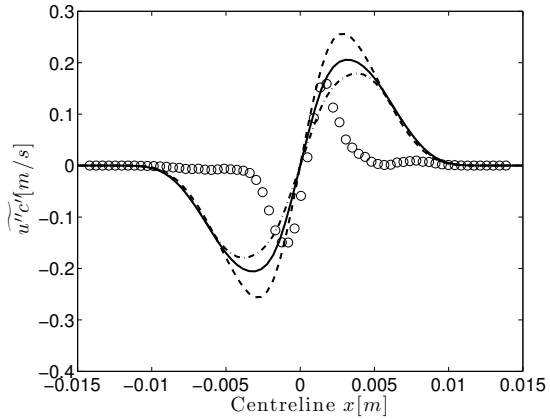

Figure 7: Predicted and measured scalar flux ($\widetilde{u''c''}$) along the centreline. Symbols and lines as Fig. 3.

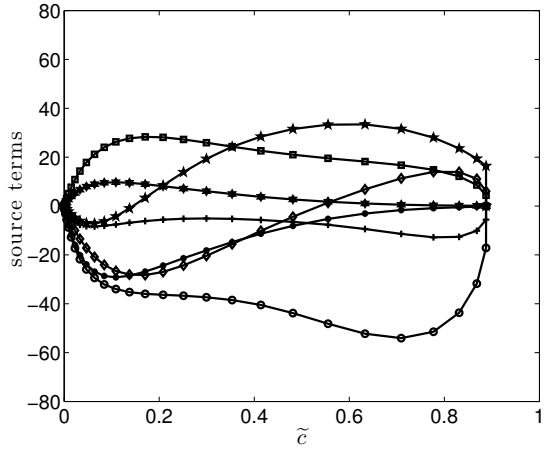

Figure 8: Source terms of predicted scalar flux ($\widetilde{u''c''}$) in the scalar field. Symbols and Lines: (-+-) Term I; (-○-) Term II; (-∗-) Term III; (-●-) Term IV; (-□-) Term V; (-◇-) Term VI; (-⋆-) Term VII.

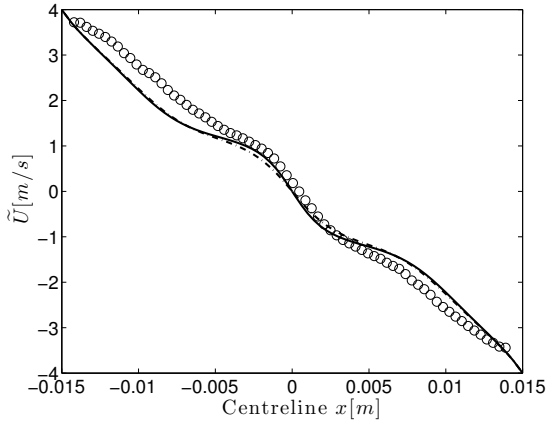

Figure 9: Predicted and measured mean velocity ($\widetilde{U}$) along the centreline. Symbols: (○) experimental data ($\phi = 0.8$) by Goh et al. [6]. Lines: (—) full second moment closures with dilatation model, $C_R = 2.6$; (-··-) full second moment closures with dilatation model, $C_R = 2.2$.

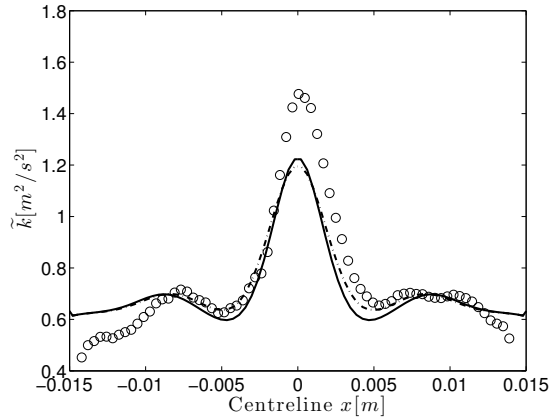

Figure 10: Predicted and measured turbulent kinetic energy ($\widetilde{k}$) along the centreline. Symbols and lines as Fig. 9.

Figs. 3 - 7. Predicted $\widetilde{k}$ along the centreline obtained by full second moment closures with the "dilatation" model provides much better agreement with experiments. Comparing with the closures without dilatation effects, the extended closures with 'dilatation" model substantially increase the turbulent kinetic energy. The normal Reynolds stresses $\widetilde{u''u''}$ and $\widetilde{v''v''}$ are shown in Figs. 4 and 5. Inspection shows that the predictions agree well with the experiment near the flame front, but that redistribution of $\widetilde{k}$ is inadequate near the stagnation plane.

A further evaluation of the predictions of scalar statistics is shown in Fig. 6, which shows the scalar variance $\widetilde{c''^2}$ along the centreline. The extended scrambling model (corresponding to the dilatation model) has a minor impact and both cases show good agreement with experimental data. The scalar flux $\widetilde{u''c''}$ is of great significance in terms of flame dynamics and non–gradient transport of $\widetilde{u''c''}$ can arise when the heat release reaches a sufficiently high value. In the current geometry, the imposed pressure gradient is causing further complications. Experimental data [6] for $\widetilde{u''c''}$ is now available and enables an assessment of the scalar flux closure. As shown in Fig. 7, the full second moment closures with reaction–related extended scrambling model (corresponding to the "dilatation" model in $\widetilde{u_i''u_j''}$) improves the prediction of the scalar flux. However, it is also apparent that further improvements are required in order to capture experimentally observed transition from gradient to non–gradient transport. The dilatation/extended scrambling models added in $\widetilde{u_i''u_j''}$ and $\widetilde{u_i''c''}$ equations, have a comparatively large impact on turbulence quantities and the turbulent scalar flux.

3.3 Sensitivity Analysis on $\widetilde{u''c''}$

Each source term of $\widetilde{u''c''}$ has been computed and analysed. Consistent with Table 1, source terms are denoted as Terms I to VII as shown in Fig. 8. It can been observed that the extended scrambling term (Term VII, corresponding to the dilatation term in $\widetilde{u_i''u_j''}$ equation) and the mean scalar gradient term (Term II) have a significantly higher impact as compared to other terms and an additional scrambling term could be required to balance the anisotropy caused by the mean scalar gradient.

As described earlier, "dilatation" and the corresponding scrambling terms in $\widetilde{u_i''u_j''}$ and $\widetilde{u_i''c''}$ equations are exact. The dilatation term in the $\widetilde{\epsilon}$ equation, however, has a modelled coefficient C_{ϵ_4}. A sensitivity analysis on C_{ϵ_4} was made and re-

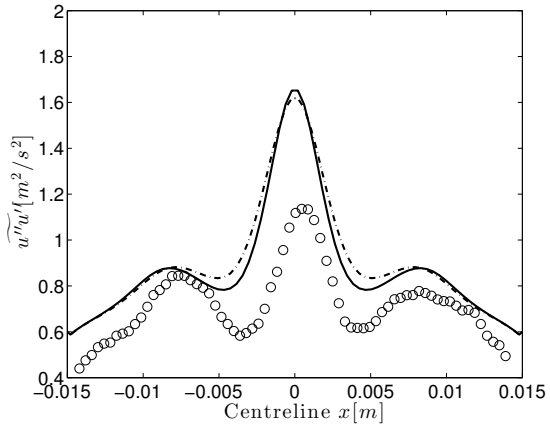

Figure 11: Predicted and measured axial Reynolds stress ($\widetilde{u''u''}$) along the centreline. Symbols and lines as Fig. 9.

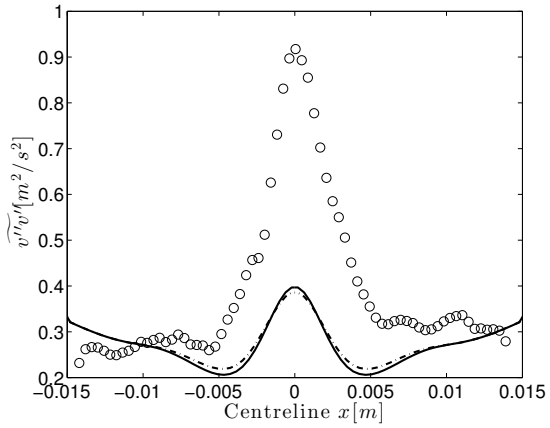

Figure 12: Predicted and measured radical Reynolds stress ($\widetilde{v''v''}$) along the centreline. Symbols and lines as Fig. 9.

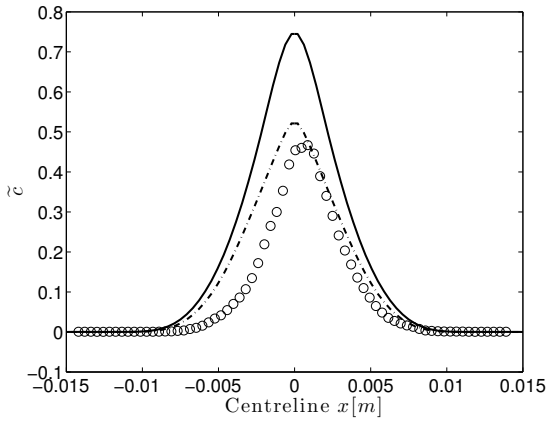

Figure 13: Predicted and measured mean reaction progress variable ($\widetilde{c}$) along the centreline. Symbols and lines as Fig. 9.

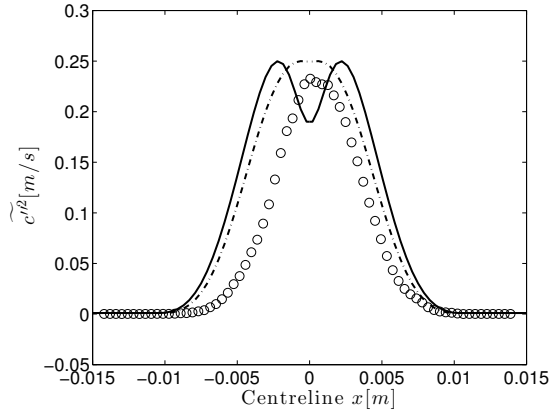

Figure 14: Predicted and measured scalar variance ($\widetilde{c''^2}$) along the centreline. Symbols and lines as Fig. 9.

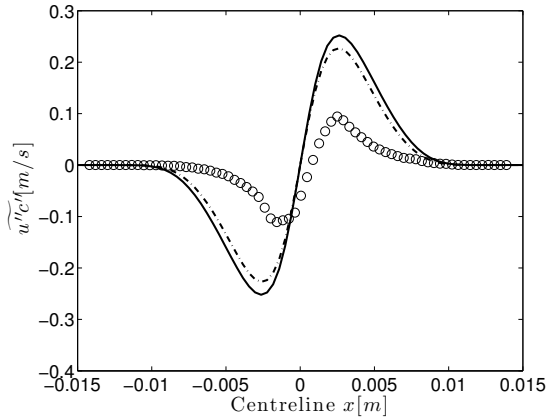

Figure 15: Predicted and measured scalar flux ($\widetilde{u''c''}$) along the centreline. Symbols and lines as Fig. 9.

veals that C_{ϵ_4} has a significant impact on $\widetilde{u''c''}$, especially near the stagnation plane. A lower value of C_{ϵ_4} leads to a lower $\widetilde{\epsilon}$ and seems to achieve better agreement for the approach to the counter-gradient. However, the shape of $\widetilde{u''c''}$ distribution along the scalar field remains problematic. The reason can arguably be related to the time scale adopted. The current simulation takes the tensor G_{ij} directly from the isothermal scrambling model with the assumption that the scalar time scale $\widetilde{\epsilon_c}/\widetilde{c''^2}$ equals to the turbulence time scale $\widetilde{\epsilon}/\widetilde{k}$. The results suggest that a lower and variable scalar time scale distribution might be expected. As Fig. 6 indicates a relatively accurate prediction of $\widetilde{c''^2}$, a more sophisticated closure for the scalar dissipation rate $\widetilde{\epsilon_c}$ may provide a fruitful direction.

As the mean scalar gradient (Term II) predicts significant anisotropy (Fig. 8), the current closure was extended by adopting an additional anisotropic scrambling term induced by the mean scalar gradient as written in Eq. 3. For all computed cases, the extended scrambling/dilatation models have been considered in both closures for the Reynolds stresses and scalar fluxes and the cofficient C_{ϵ_4} in turbulent kinetic energy dissipation equation is taken as 1.0. For the cases using Eq. 3, the coefficient C_{3c} varies from 0.25 to 0.80. Closures with the mean scalar gradient induced scrambling term decrease the absolute value of $\widetilde{u''c''}$. Thus, an additional term corresponding to the mean scalar gradient should be examined more thoroughly and considered in the closure for the scrambling term.

3.4 Effects of Chemical Reaction

The chemical reaction rate closure based on the laminar flamelet assumption is comparatively simple and the accuracy can be expected to be reduced by local extinction effects near the flammability limits. Accordingly, methane–air flames with an equivalence ratio of 0.80 was also studied. The standard dissipation equation with preferential acceleration and dilatation additions were used as the impact of the renormlization theory based modification to the dissipation rate equation [14] has a comparatively modest impact in the current flames.

Predicted and measured results are shown in Figs. 9 - 15. The chemical reaction rate coefficient C_R was chosen as the standard value (2.6) and also reduced to 2.2. It is evident that the chemical reaction rate has a significant impact as shown in Figs. 13 - 15. The case with $C_R = 2.6$ can no longer predict the mean reaction progress variable and the position of the flame front as accurately as for the richer case. Better agreement is achieved using the lower value, suggesting that local extinction effects need to be taken into account.

4. Conclusion

The present study is based on a comprehensive second moment closure for premixed turbulent flames with variable density effects. The closures for the pressure correlation terms have been modelled thoroughly. In addition to the preferential acceleration terms associated with the mean pressure gradient, the dilatation and extended scrambling terms induced by the fluctuating pressure have also been considered. The choice of the latter is consistent with the chemical reaction closure implied by BML formalism. The complete closures have been applied to the simulation of turbulent opposed premixed methane–air flames. Encouraging agreements with experimental data suggest that the dilatation model has a significant impact. However, the modelling of $\widetilde{k}$ redistribution appears to need further consideration due to the inaccurate prediction of $\widetilde{u''u''}$ and $\widetilde{v''v''}$ near the stagnation plane. With regard to the scalar statistics, the full second moment closure predicts the scalar variance $\widetilde{c''^2}$ accurately and using an extended scrambling term (Term VII) provides a slightly better prediction on the $\widetilde{u''c''}$. Further analysis of the $\widetilde{u''c''}$ transport equation suggests that a transport of the scalar dissipation rate $\widetilde{\epsilon_c}$ should be considered along with a scaling on the mean scalar gradient in the scrambling term.

Results also suggest that inclusion of local extinction effects becomes necessary near the flammability limits.

Acknowledgements

Lu Tian would like to acknowledge the support of Imperial College PhD Scholarship and discussions with Henry Goh, Fabian Hampp and Vangelis Váos.

References

[1] C.G. Speziale, S. Sarkar, T.B. Gatski, J. Fluid Mech. (1991) 227-245.

[2] R.P. Lindstedt, E.M. Váos, Combust. Flame 116 (1999) 461-485.

[3] W.P. Jones, B.E. Launder, Int. J. Heat Mass Tran. 15 (1972) 301-314.

[4] P.A. Libby, K.N. Bray, AIAA J. 19(2) (1981) 205-213.

[5] E. Mastorakos, Turbulent Combustion in Opposed Jet Flows, PhD thesis, University of London, 1993.

[6] K.H.H. Goh, P. Geipel, R.P. Lindstedt, Combust. Flame 161 (2014) 2419-2434.

[7] H. Pitsch, Annu. Rev. Fluid Mech. 38 (2006) 453-482.

[8] S.W. Zhang, C.J. Rutland. Combust. Flame 162 (1995) 447-461.

[9] T. Hůlek, R.P. Lindstedt, Mathl. Comput. Modelling 24(8) (1996)137-147.

[10] K.N.C. Bray. P.A. Libby, J.B. Moss, Combust. Flame 61 (1985) 87-102.

[11] B.E. Launder, B.I. Sharma, Letters in Heat and Mass Transfer 1(2) (1974) 131-137.

[12] W.P. Jones, Turbulence Modelling for Combusting Flows. Modelling for Combustion and Turbulence. Lecture Series 1992-2003, von Karman Institute for Fluid Dynamics (1992).

[13] B.J. Daly, F.H. Harlow, Phys. Fluids 13 (1970) 2634.

[14] V. Yakhot, S.A. Orszag, Phys. Fluids 4(7) (1992) 1510-1520.

[15] R.K. Robinson, R.P. Lindstedt, Combust. Flame 158 (2011) 666-686.

[16] P. Geipel, K.H.H. Goh, R.P. Lindstedt, Flow Turbul. Combust. 85 (2010) 397-419.

[17] R.I. Issa, J. Com. Phys. 62(1) (1986) 40-65.

[18] P.K. Sweby, SIAM J. Numerical Anal. 21(5) (1984) 995-1011.

Table 1: Table of modeled governing equations
(the tensor G_{ij} and symbols are consistent with [2])

$$\frac{\partial \bar{\rho}}{\partial t} + \frac{\partial \bar{\rho}\widetilde{u}_l}{\partial x_l} = 0$$

$$\frac{\partial \bar{\rho}\widetilde{u}_i}{\partial t} + \frac{\partial \bar{\rho}\widetilde{u}_l\widetilde{u}_i}{\partial x_l} = -\frac{\partial p}{\partial x_i} - \frac{\partial \bar{\rho}\widetilde{u_i'' u_l''}}{\partial x_l}$$

$$\frac{\partial \bar{\rho}\widetilde{c}}{\partial t} + \frac{\partial \bar{\rho}\widetilde{u}_l\widetilde{c}}{\partial x_l} = -\frac{\partial \bar{\rho}\widetilde{u_l'' c''}}{\partial x_l} + \bar{S}_c$$

$$\bar{S}_c = C_R \rho_u \frac{u_L}{v_K}\frac{\widetilde{\epsilon}}{\widetilde{k}}\widetilde{c}\left(1-\widetilde{c}\right) \;\; C_R = 2.6$$

$$\frac{\partial \bar{\rho}\widetilde{u_i'' u_j''}}{\partial t} + \frac{\partial \bar{\rho}\widetilde{u}_l\widetilde{u_i'' u_j''}}{x_l} = \frac{\partial}{\partial x_k}\left[C_s \bar{\rho}\frac{\widetilde{k}}{\widetilde{\epsilon}}\widetilde{u_k'' u_l''}\frac{\partial \widetilde{u_i'' u_j''}}{\partial x_l}\right] + P_{ij} + \Phi_{ij} + \phi_{ij}^D + \phi_{ij}^{CD} + \phi_{ij}^A - \bar{\rho}\epsilon_{ij}$$

$$P_{ij} = -\bar{\rho}\left[\widetilde{u_i'' u_l''}\frac{\partial \widetilde{u}_j}{\partial x_l} + \widetilde{u_j'' u_l''}\frac{\partial \widetilde{u}_i}{\partial x_l}\right]$$

$$\Phi_{ij} = \left[\overline{u_i''}\frac{\partial \bar{p}}{\partial x_j} + \overline{u_j''}\frac{\partial \bar{p}}{\partial x_i}\right] \;\; C_s = 0.22$$

$$\phi_{ij}^D = \frac{2}{3}\delta_{ij}\left\langle p'\frac{\partial u_k''}{\partial x_k}\right\rangle = \underbrace{\frac{1}{3}\delta_{ij}\left(\tau u_L\right)^2 \overline{S_c}\left(\langle c\rangle - \frac{1}{2}\right)}_{\text{Dilatation Term}}$$

$$\phi_{ij}^{CD} + \phi_{ij}^A - \bar{\rho}\epsilon_{ij} = \bar{\rho}G_{ik}\widetilde{u_k'' u_j''} + \bar{\rho}G_{jk}\widetilde{u_k'' u_i''} + \bar{\rho}C_o\delta_{ij}\widetilde{\epsilon} + C_{A_R}\left[\Phi_{ij} - \frac{1}{3}\delta_{ij}\Phi_{kk}\right] \;\; C_o = 2.1 \;\; C_{A_R} = -0.30$$

$$\frac{\partial \bar{\rho}\widetilde{u_i'' c''}}{\partial t} + \frac{\partial \bar{\rho}\widetilde{u}_l\widetilde{u_i'' c''}}{x_l} = \frac{\partial}{\partial x_k}\left[C_s \bar{\rho}\frac{\widetilde{k}}{\widetilde{\epsilon}}\widetilde{u_k'' u_l''}\frac{\partial \widetilde{u_i'' c''}}{\partial x_l}\right] - \underbrace{\left[\bar{\rho}\widetilde{u_l'' c''}\frac{\partial \widetilde{u}_i}{\partial x_l}\right]}_{\text{Term I}} + \underbrace{\left[\bar{\rho}\widetilde{u_i'' u_l''}\frac{\partial \widetilde{c}}{\partial x_l}\right]}_{\text{Term II}} - \underbrace{\overline{c''}\frac{\partial \bar{p}}{\partial x_i}}_{\text{Term III}} + \underbrace{\bar{\rho}G_{il}\widetilde{u_l'' c''}}_{\text{Term IV}} + \underbrace{\frac{\overline{S_c}}{\widetilde{c''^2}}\left(\frac{1}{2} - \widetilde{c}\right)\widetilde{u_i'' c''}}_{\text{Term V}}$$

$$\underbrace{-C_{A_S}\overline{c''}\frac{\partial \bar{p}}{\partial x_i}}_{\text{Term VI}} + \underbrace{\frac{1}{2}\left(\tau u_L\right)\overline{S_c}\left(\langle c\rangle - \frac{1}{2}\right)}_{\text{Term VII: Extended Scrambling Term}} \quad C_{A_S} = -1/3$$

$$\frac{\partial \bar{\rho}\widetilde{\epsilon}}{\partial t} + \frac{\partial \bar{\rho}\widetilde{u}_l\widetilde{\epsilon}}{x_l} = \frac{\partial}{\partial x_k}\left[C_{s_\epsilon}\bar{\rho}\frac{\widetilde{k}}{\widetilde{\epsilon}}\widetilde{u_k'' u_l''}\frac{\partial \widetilde{\epsilon}}{\partial x_l}\right] - C_{\epsilon_1}\frac{\widetilde{\epsilon}}{\widetilde{k}}\widetilde{u_k'' u_l''}\frac{\partial \widetilde{u_k}}{\partial x_l} - C_{\epsilon_2}\frac{\widetilde{\epsilon}}{\widetilde{k}}\widetilde{\epsilon} - C_{\epsilon_3}\frac{\widetilde{\epsilon}}{\widetilde{k}}\overline{u_l''}\frac{\partial \bar{p}}{\partial x_l} + \underbrace{C_{\epsilon_4}\left(\frac{1}{2}\left(\tau u_L\right)^2\overline{S_c}\left(\langle c\rangle - \frac{1}{2}\right)\right)}_{\text{Dilatation Term}}$$

$$C_{\epsilon_1} = 1.44, \;\; C_{\epsilon_2} = 1.92, \;\; C_{\epsilon_3} = 1.20, \;\; C_{S_\epsilon} = 0.18, \;\; C_{\epsilon_4} = 1.00$$